

Design parameters for a nano-optical Yagi-Uda antenna

Holger F. Hofmann, Terukazu Kosako and Yutaka Kadoya

Graduate School of Advanced Sciences of Matter, Hiroshima University, Kagamiyama 1-3-1, Higashi Hiroshima 739-8530, Japan

Abstract. We investigate the possibility of directing optical emissions using a Yagi-Uda antenna composed of a finite linear array of nanoparticles. The relevant parameters characterizing the plasma resonances of the nanoparticles are identified and the interaction between the array elements is formulated accordingly. It is shown that the directionality of the optical emission can be observed even in the presence of non-negligible absorption losses in the nanoparticles. We conclude that a finite array of gold nanorods may be sufficient for the realization of a working nano-optical Yagi-Uda antenna.

PACS numbers: 78.67.-n 42.82.-m 84.40.Ba

E-mail: h.hofmann@osa.org

1. Introduction

Nanoscience is essentially the art of applying engineering principles at scales where some of our conventional assumptions cease to be valid. One interesting example is the control of light using the plasma resonances of metallic nanoparticles. The optical response of metal nanoparticles is well described by classical electrodynamics, with the material properties represented by the frequency dependent dielectric constant. It is therefore possible to apply ideas from electrical engineering directly to the design of nano-optical devices [1]. However, the optical response of metals is quite different from the metallic conductivity observed low frequencies. One well researched consequence of this difference is the observation of resonant excitations known as surface plasmons in nanoparticles much smaller than the optical wavelength [2]. Such resonances can be used to enhance and direct the spontaneous emission of light by single molecules, quantum dots, or similar point-like light sources, just like an appropriately designed resonant antenna can enhance and direct radio emissions [3, 4]. Recently, this idea has been combined with the principles of antenna design known from radio and microwave technology, resulting in the experimental realizations of nano-optical equivalents of half-wave and bow-tie antennas [5, 6, 7, 8]. Based on these advances in the fabrication of nano-optical antennas, it seems only natural to ask whether the same principles can be used to also achieve the highly directional emission of radio antennas in the optical regime.

At radio frequencies, high directionality can be obtained by conventional Yagi-Uda antennas consisting of a reflector and several directors arranged in line around the feed. In the optical regime, the same kind of antenna structure could be realized by a linear array of nanoparticles. In our recent work, we therefore pointed out the possibility of using a nano-optical Yagi-Uda antenna made of metal nanorods to direct the optical emission from systems such as molecules, quantum dots or optical semiconductors [9]. A similar proposal based on concentric core-shell nanoparticles was developed independently by Jingjing Li et al. at the University of Pennsylvania [10].

Since there appears to be a growing interest in this kind of device structure, it may be useful to formulate the essential theory of Yagi-Uda antennas in an accessible manner. In the following, we therefore develop a simple theory of the nano-optical Yagi-Uda antenna that allows us to identify the relevant properties of the nanoparticles and their effect on the directivity of the emission. To do so, we have to consider both the basic electrodynamics of near field coupling between dipoles at distances close to the wavelength of their emission (section 2), and the interaction between the fields and the material properties inside each nanoparticle (section 3). The result allows us to estimate the relevant antenna parameters for gold nanorods embedded in a glass substrate (section 4). We then apply the near field coupling equations of section 2 to derive the emission pattern of Yagi-Uda antenna arrays (section 5) and use the results to optimize the detuning and the array spacings of a five element antenna array (section 6). Finally, we investigate the effect of non-negligible absorption losses on the emission

pattern (section 7) and show that the directivity of the emission is sufficiently robust against the losses expected for the gold nanorods described in section 4.

2. Near field interactions and radiative damping

In order to have a maximal effect on the emission pattern, antenna elements must be placed at distances comparable to the wavelength λ of the emitted radiation. Therefore, the interaction between the elements is described by the electric field in the transitional range between the quasi-static dipole near field and the far field. For an oscillating dipole d emitting radiation of wavelength λ into a homogeneous medium of dielectric constant $\epsilon_{\text{med.}}$, the field pattern is determined by Hertz's solution of electric dipole radiation. At a distance of r perpendicular to the orientation of the oscillating dipole, the electric field can then be given as

$$E_z(x; A) = -\frac{3}{2}A\frac{1}{x^3}(i + x - ix^2)\exp(ix),$$

where

$$A = -i\frac{4\pi^2d}{3\epsilon_{\text{med.}}\lambda^3} \quad \text{and} \quad x = 2\pi\frac{r}{\lambda}. \quad (1)$$

The parameter A expresses the dipole in terms of its radiation damping field (that is, its self-interaction). This representation of the dipole greatly simplifies the representation of polarizability. For a resonant oscillator without internal losses, the incoming field E_{in} is exactly compensated by the radiation damping field of the induced dipole. Therefore, the dipole of a resonant loss free nanoparticle is determined by $A = -E_{\text{in}}$. In the more general case of a finite detuning and additional absorption losses, the scaled response function can be expressed as

$$A = -\frac{E_{\text{in}}}{1 + \gamma + i\delta}, \quad (2)$$

where δ and γ describe the effects of detuning and of absorption losses as ratios of the associated fields to the radiation damping field of the dipole.

Equations (1) and (2) describe the coupling effects in any linear dipole array at any wavelength. The material properties of the system are summarized by the two parameters γ and δ , describing the losses and the spectral properties of the array elements. The possibility of designing a nano-optical Yagi-Uda antenna therefore depends mainly on the ability to control these two parameters of the individual nanoparticles.

3. Optical properties of the nanoparticles

A major difference between nano-optical antennas and radio frequency antennas is that the plasma resonance of a metallic nanoparticle is nearly independent of size. In principle, the elements of an antenna array can therefore be much smaller than the half wavelength size of classical antenna designs [6]. The reason for this size independence

is that the role of the inductance of the classical antenna is taken over by the mass of the free electrons in the plasma oscillation. This effect of the electron mass is reflected by the negative real part of the dielectric constants of metals at optical frequencies, which converts the conventional capacitive effect of polarizability into an inductive effect [1]. The polarization P of a nanoparticle by an incoming field E_{in} can thus be described in close analogy to the response of an electrical circuit to the application of a voltage. Specifically, the response can be separated into the response of the material inside the particle described by the complex dielectric constant $\epsilon_{\text{particle}} = \epsilon_r \epsilon_{\text{med.}}$, the shape dependent field of the surface charges accumulated at the interface between the nanoparticle and the surrounding medium, and the radiation damping field caused by the emission of the total dipole $d = PV$, where V is the volume of the nanoparticle. The relation between incoming field and polarization then reads

$$E_{\text{in}} = \underbrace{\frac{1}{(\epsilon_r - 1)\epsilon_{\text{med.}}}}_{\substack{\text{material} \\ \text{(inductive)}}} P + \underbrace{\frac{N}{\epsilon_{\text{med.}}}}_{\substack{\text{shape} \\ \text{(capacitive)}}} P - i \underbrace{\frac{4\pi^2 V}{3\epsilon_{\text{med.}} \lambda^3}}_{\substack{\text{radiation} \\ \text{(resistive)}}} P. \quad (3)$$

Here, the capacitive effect of the surface charge is given in terms of the depolarization factor N , which is defined in close analogy to the demagnetization factor in the magnetic response of a particle as the factor by which a polarization P weakens the electric field E inside a body of a given shape. In its more conventional form, the polarization of a nanoparticle is given as

$$P = \frac{(\epsilon_r - 1)\epsilon_{\text{med.}} E_{\text{in}}}{1 + N(\epsilon_r - 1) - i(\epsilon_r - 1)R}, \quad \text{where} \quad R = \frac{4\pi^2 V}{3\lambda^3}. \quad (4)$$

This equation is equivalent to the antenna response equation (2) in section 2, where P is expressed in terms of the radiation damping field, $A = -iRP/\epsilon_{\text{med.}}$. We can therefore identify the parameters γ and δ in eq.(2) with the corresponding terms in eq.(4) to find the relative losses γ and the effective detuning δ of a nanoparticle based on its dielectric constant $\epsilon_r = \epsilon_{\text{particle}}/\epsilon_{\text{med.}}$, its volume V (given in terms of the scaled parameter R), and its depolarization factor N . The results read

$$\gamma = \frac{1}{R} \frac{\text{Im}(\epsilon_r)}{|\epsilon_r - 1|^2} \quad (5)$$

$$\delta = \frac{1}{R} \left(N + \frac{\text{Re}(\epsilon_r - 1)}{|\epsilon_r - 1|^2} \right). \quad (6)$$

Using these relations, we can now determine whether a specific type of nanoparticle is suitable for the construction of an antenna array.

4. Shape and size dependences for gold nanoparticles embedded in glass

One simple and convenient way to realize a nano-optical Yagi-Uda antenna may be to use gold nanoparticles embedded in a glass substrate. The optical properties of gold nanoparticles are well known and the dielectric constants at different frequencies is

Table 1. Optical properties of gold nanorods embedded in a glass substrate with a dielectric constant of $\epsilon_{\text{med.}} = 2.3$.

Wavelength in vacuum	$\epsilon_{\text{particle}}$ of gold [11]	Wavelength in glass, λ	$\epsilon_r - 1$
582 nm	-8.11+i 1.66	384 nm	-4.53 + i 0.72
617 nm	-10.7+i 1.37	407 nm	-5.65 + i 0.60
660 nm	-13.6+i 1.04	435 nm	-6.91 + i 0.45
705 nm	-16.8+i 1.07	465 nm	-8.30 + i 0.47
756 nm	-20.6+i 1.27	499 nm	-9.96 + i 0.55
821 nm	-25.8+i 1.63	541 nm	-12.2 + i 0.71

Table 2. Volume dependence of losses for gold nanoparticles embedded in a glass substrate.

Wavelength in vacuum (glass)	γR	$V(\gamma = 1)$
582 nm ($\lambda = 384$ nm)	3.42×10^{-2}	$2.6 \times 10^{-3} \lambda^3$
617 nm ($\lambda = 407$ nm)	1.86×10^{-2}	$1.4 \times 10^{-3} \lambda^3$
660 nm ($\lambda = 435$ nm)	1.20×10^{-2}	$9.1 \times 10^{-4} \lambda^3$
705 nm ($\lambda = 465$ nm)	6.80×10^{-3}	$5.2 \times 10^{-4} \lambda^3$
756 nm ($\lambda = 499$ nm)	5.53×10^{-3}	$4.2 \times 10^{-4} \lambda^3$
821 nm ($\lambda = 541$ nm)	4.75×10^{-3}	$3.6 \times 10^{-4} \lambda^3$

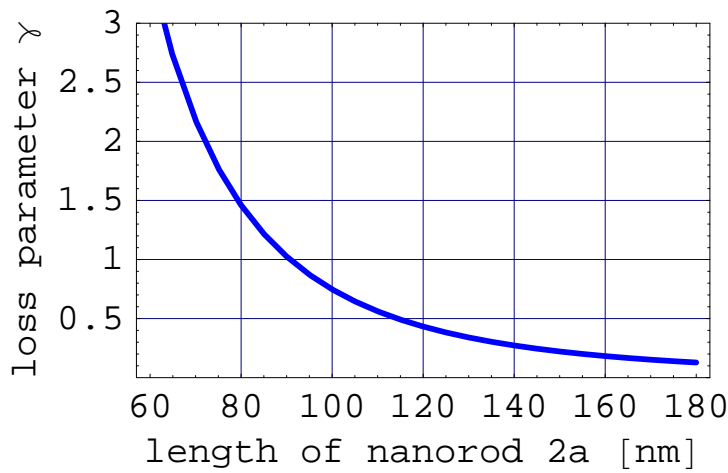
readily available [11]. We have used this data to determine the optical properties of gold nanoparticles in a glass substrate with a dielectric constant of $\epsilon_{\text{med.}} = 2.3$. Table 1 shows the wavelengths inside the glass and the values of $\epsilon_r - 1$ that determine the dependence of the loss and detuning parameters on the size and shape of the nanoparticles.

The main limitations on realizing a nano-optical antenna array with gold particles arises from the absorption losses represented by the imaginary part of the dielectric constant ϵ_r describing the optical response of gold relative to the surrounding glass. According to eq.(5), the relevant loss parameter γ is given by the ratio of material properties and the volume of the nanoparticle. It is therefore possible to compensate the absorption losses of the material by making the volume of the nanoparticle larger. The volume at which the loss parameter γ becomes one may be used as a reference point for an estimate of the necessary particle size. Table 2 illustrates this volume dependence of the losses by giving the product of losses and scaled volume γR , as well as the volume at which the loss parameters is $\gamma = 1$ in terms of the cubic wavelength in glass. The results indicate that the dimensions of the antenna elements should be of the order of a tenth of the wavelength inside the medium. This is still small enough to justify the approximation as a local dipole oscillator, while also being large enough to permit a definition of the device structure by standard lithographic techniques.

Once the size has been fixed, the precise detuning can be determined by varying the shape. The relation between the detuning parameter δ and the depolarization factor N

Table 3. Depolarization factors for resonant antenna elements and the corresponding aspect ratios for the case of ellipsoids.

Wavelength in vacuum (glass)	$N(\delta = 0)$	Aspect ratio a/b
582 nm ($\lambda = 384$ nm)	0.215 (about 1/5)	1.63
617 nm ($\lambda = 407$ nm)	0.175 (about 1/6)	1.99
660 nm ($\lambda = 435$ nm)	0.144 (about 1/7)	2.37
705 nm ($\lambda = 465$ nm)	0.120 (about 1/8)	2.76
756 nm ($\lambda = 499$ nm)	0.100 (exactly 1/10)	3.21
821 nm ($\lambda = 541$ nm)	0.082 (about 1/12)	3.75

**Figure 1.** Length dependence of the loss parameter γ for an elliptical gold nanorod of aspect ratio 2.76 at its resonant wavelength of 705 nm.

is given by eq. (6). The depolarization factor can be adjusted by varying the aspect ratio of the nanoparticle, defined as the ratio of the length a along the direction of the electric field and the perpendicular width b . For the case of an ellipsoid, analytical formulas are known from the study of demagnetization [12], and these can be used to estimate the approximate aspect ratios for nanorods tuned to a specific frequency. However, the exact relation between the depolarization factor N and the aspect ratio may depend on details of the shape, so it may be best to obtain it experimentally for any given geometry. Table 3 shows the depolarization factor necessary to establish resonance at each of the frequencies given in table 1, together with the corresponding aspect ratio for an ellipsoid.

We can now get a practical idea of the relation between the loss parameter γ and the size of the nanoparticles used to construct the antenna by relating γ to the length of an ellipsoid with the appropriate aspect ratio. Fig.1 shows the dependence of losses on length for a particle of aspect ratio 2.76 at its resonant wavelength of 705 nm. A loss parameter of $\gamma = 0.5$ is obtained for particles with a length of $2a = 115$ nm,

corresponding to 0.25λ inside glass ($\lambda = 465\text{nm}$). To obtain a loss parameter of $\gamma = 0.1$, the length of the gold nanorods must be increased to $2a = 0.42\lambda$, or about 195 nm. For gold nanoparticles sufficiently shorter than the half wavelength of classical antennas, it is therefore unrealistic to neglect the effects of losses on the performance of the antenna. However, losses around $\gamma = 0.5$ are still reasonably low, so particles of about 100 nm may be suitable for use in an antenna array.

In order to construct a Yagi-Uda antenna, it is also necessary to control the detuning parameter δ of the elements used as directors. As eq.(6) shows, the detuning caused by a change of ΔN in the detuning factor is equal to $\Delta N/R$. We can therefore determine the change in depolarization factor required to achieve the intended detuning δ by multiplying δ with R . For example, an antenna element operating at 705 nm with losses of $\gamma = 0.5$ can be detuned to $\delta = 1$ by increasing the depolarization factor to $0.120 + R = 0.136$. This depolarization factor corresponds to an aspect ratio of about 2.5 for ellipsoids. Using the volume corresponding to losses of $\gamma = 0.5$ at 705 nm, this aspect ratio defines a length of $2a = 107$ nm for the ellipsoid. Roughly speaking, a reduction of 7% in length thus corresponds to an increase of one in the detuning parameter δ .

5. Coupled dipole theory of the antenna array

The operating principle of the Yagi-Uda antenna is based on the observation that capacitively detuned antenna elements effectively guide the emissions from a neighboring feed towards their direction, while resonant or inductively detuned elements always reflect the emissions back towards the feed. A Yagi-Uda antenna therefore consists of an array of several directors placed in front of the feed, and one or two reflectors behind the feed. At radio frequencies, the description of a Yagi-Uda antenna is usually complicated by the fact that the length of the antenna rods exceeds the distance between antenna elements. It is then unrealistic to assume a simple dipole coupling interaction, such as the one given by eq. (1). However, in the case of nanoparticles, the dipole coupling approximation is usually sufficient to describe interactions in an array [13, 14]. A nano-optical Yagi-Uda antenna can therefore be described in terms of the fundamental physics of an interacting dipole chain using the formalism developed in section 2.

In the following, we will consider a number of antenna elements at positions x_n along the antenna axis around a feed at $x = 0$. As in eq. (1), all distances are given in units of $\lambda/(2\pi)$. The feed is a light emitting system such as a molecule or quantum dot, oscillating at a well defined frequency. The dipole amplitude of the feed oscillation is given by A_F . Each passive antenna elements responds to this feed oscillation with a dipole amplitude A_n proportional to A_F . The precise interactions are defined by eqs.(1) and (2). They form a system of N linear equations, where N is the number of passive elements of the antenna array,

$$A_n = \frac{1}{1 + \gamma_n + i\delta_n} \left(E_z(|x_n|; A_F) + \sum_{m \neq n} E_z(|x_n - x_m|; A_m) \right). \quad (7)$$

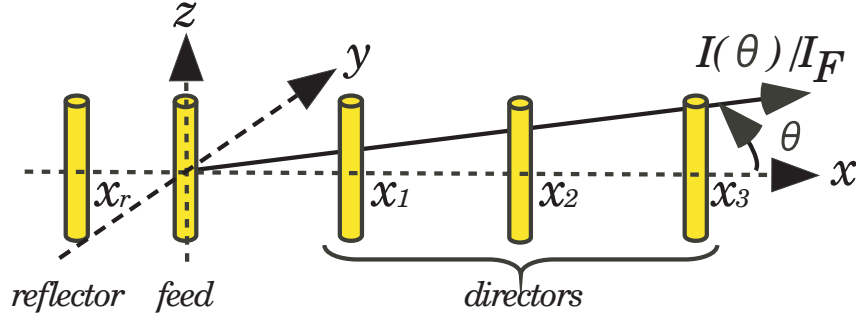


Figure 2. Sketch of a five element Yagi-Uda antenna, indicating the positions of the reflector, feed, and directors, and the angle of emission θ in the plane orthogonal to the dipoles of the antenna elements.

By solving this system of linear equations for a particular configuration of antenna elements, we can determine the ratio between the dipole amplitudes A_n and the feed amplitude A_F . From these amplitudes, we can then derive the far field emission pattern. In the plane orthogonal to the dipoles, this pattern is given by

$$I(\theta)/I_F = \left(\left| 1 + \sum_n \frac{A_n}{A_F} \exp(-ix_n \cos(\theta)) \right|^2 \right), \quad (8)$$

where θ is the angle between the axis of the antenna array and the emission direction and I_F is the intensity of emission from a single dipole oscillating at the feed amplitude A_F .

6. Basic structure of a five element Yagi-Uda antenna

Fig. 2 illustrates the basic structure of a five element Yagi-Uda antenna. It consists of a resonant reflector at $x_r < 0$ ($\delta_r = 0$), the feed at $x = 0$, and three equally spaced directors at $x_1 = x_a$, $x_2 = 2x_a$, and $x_3 = 3x_a$, capacitively detuned by $\delta = \delta_1 = \delta_2 = \delta_3$. A typical choice of parameters for radio frequency antennas is $x_r = -1.4$ corresponding to a reflector distance of 0.22λ , $x_a = 2$ corresponding to a director spacing of λ/π , and a detuning parameter of $\delta = 1$. However, the exact choice of parameters is not very critical, making a Yagi-Uda antenna very robust against misalignments of its elements.

Fig. 3 shows the emission pattern of an antenna with the above parameters in the limit of negligible absorption losses ($\gamma_n = 0$ for all elements). As expected for a highly directional antenna, most of the emission is concentrated in a single lobe around $\theta = 0$. In addition, two much smaller sidelobes exist around angles of $\theta = \pm 1.25$ ($\pm 72^\circ$). The width of the main lobe can be estimated by using the half angle $\theta_{1/2}$, defined as the angle between the directions along which the emission intensity is half of the peak intensity. In the present case, $I(\theta)/I(0) = 1/2$ at $\theta = \pm 0.46$, so the half angle is $\theta_{1/2} = 0.92$ (53°). Compared to the emission of a dipole of amplitude A_F , the forward emission is enhanced by a factor of $I(0)/I_F = 5.9$ and the backward emission is suppressed by $I(\pi)/I_F = 0.13$.

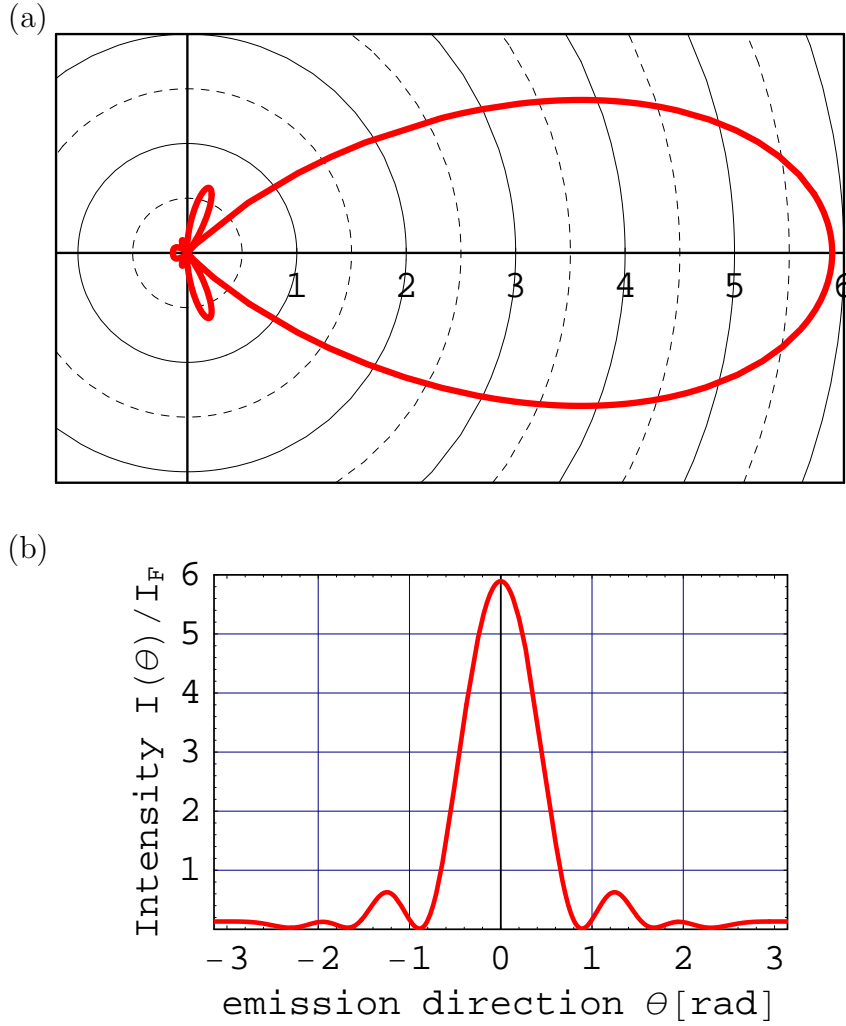


Figure 3. Emission pattern of an antenna with negligible losses. (a) shows the polar plot and (b) shows the rectangular plot. The antenna parameters are $x_r = -1.4$, $x_a = 2$, $\delta = 1$ and $\gamma_n = 0$.

To illustrate the effects of the antenna parameters on the directionality of the emission, we have determined the emission patterns for different detuning and director spacings. Fig. 4 shows the effect of changing the detuning parameter δ on the emission of a five element antenna with $x_r = -1.4$, $x_a = 2$, and $\gamma_n = 0$. The importance of capacitive detuning can be seen clearly in the sharp increase in forward emission enhancement $I(0)/I_F$, and in the simultaneous reduction in half angle $\theta_{1/2}$ at a detuning of about $\delta = 0.5$. The forward enhancement reaches a maximum of about 6.5 around $\delta = 1.2$, and then drops off gradually. On the whole, the results indicate that it is better to detune too much than to detune too little, with nearly equally good antenna patterns for detunings in the range of $\delta = 1$ to $\delta = 2.5$.

Fig. 5 shows the effect of changing the antenna spacing x_a on the emission of a five element antenna with $x_r = -1.4$, $\delta = 1$, and $\gamma_n = 0$. As one might expect for

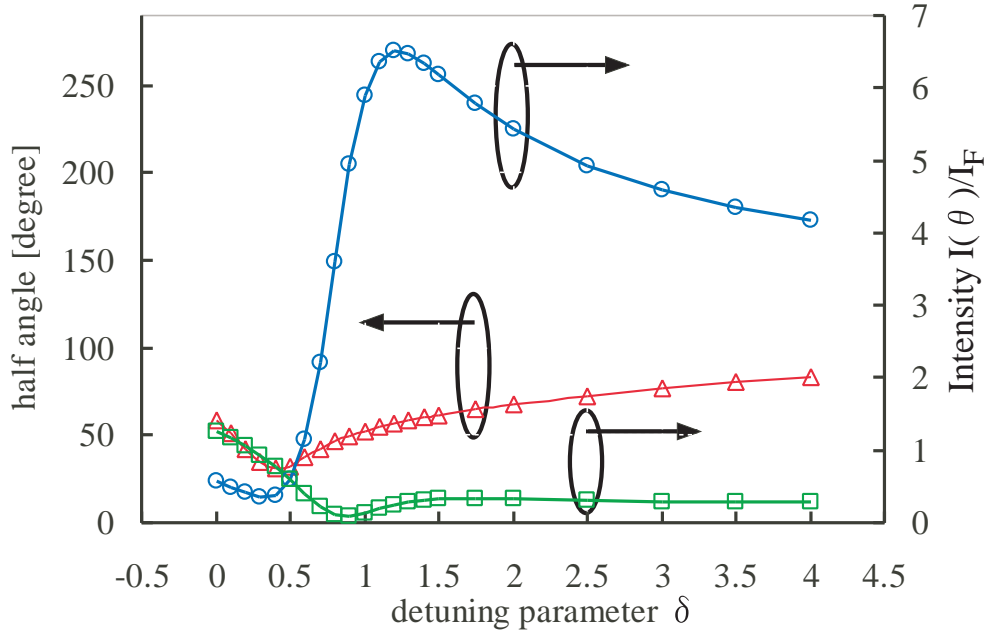


Figure 4. Dependence of antenna emission on the detuning parameter δ of the directors. The blue line shows the enhancement of forward emission, $I(0)/I_F$, the green line shows the suppression of backward emission, $I(\pi)/I_F$, and the red line shows the half angle $\theta_{1/2}$ of the forward emission.

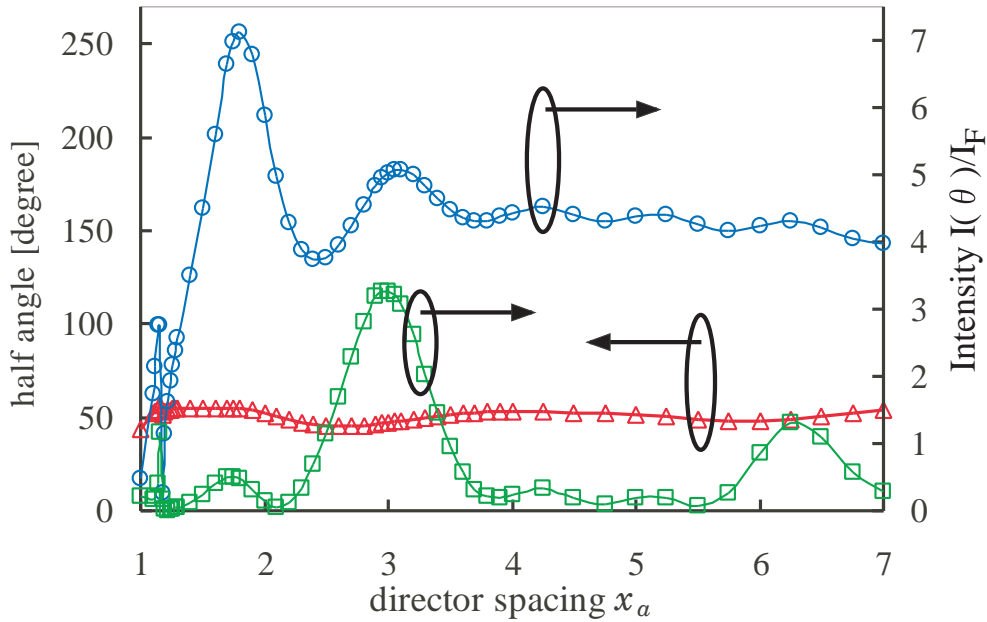


Figure 5. Dependence of antenna emission on director spacing x_a . The blue line shows the enhancement of forward emission, $I(0)/I_F$, the green line shows the suppression of backward emission, $I(\pi)/I_F$, and the red line shows the half angle $\theta_{1/2}$ of the forward emission.

the emission characteristics of an array, the dependence on array spacing shows some periodic features. However, both forward and backward emissions oscillate together, so that a spacing of $x_a = 3$ corresponding to half a wavelength causes an enhancement of backward emission $I(\pi)/I_F$ that is almost as big as the enhancement of forward emission. These conditions are much better at $x_a = 1.8$, where the forward emission is maximally enhanced by a factor of about 7.2, whereas the backward emission is suppressed by about 0.5. A good combination of enhanced forward emission and strongly suppressed backward emission can be obtained at $x_a = 2$ and at $x_a = 1.6$, corresponding to the array spacings of λ/π and $\lambda/4$ commonly found in radio frequency antennas.

Interestingly, it is also possible to obtain acceptable antenna patterns at much wider spacings. In particular, the whole range of director spacings from $x_a = 4$ to $x_a = 5.5$ exhibits very similar radiation patterns with forward enhancements of about 4 and half angles of about $\theta_{1/2} = 0.9$ (51°). It may thus be possible to build antennas with director spacings of about three quarters of a wavelength that will work even if the resonant wavelength is shifted considerably. However, such long antenna structures usually have more sidelobes at angles between $\theta = 0$ and $\theta = \pi$, so we will focus on the more conventional case of the $x_a = 2$ array in the following.

7. Emission characteristics of nano-optical Yagi-Uda antennas with non-negligible absorption losses

As we have seen in section 4, it may be difficult to achieve negligible losses in plasmonic nanoparticles. Specifically, an antenna made of 100 nm long gold nanorods embedded in glass is expected to have a loss parameter of about $\gamma = 0.5$. In the following, we therefore present the emission patterns of antennas with non-negligible absorption losses.

Fig. 6 shows the emission pattern for a Yagi-Uda antenna with $\gamma_n = 0.5$ for all elements. The director detuning has been increased to $\delta = 1.5$ to preserve the ratio of δ and $1 + \gamma$ in eq.(7). The array parameters are $x_r = -1.4$ and $x_a = 2$, the same as in fig. 3. Compared to the loss free case shown in that figure, the enhancement of forward emission has dropped by one half to $I(0)/I_F = 3$, and the suppression of backward emission is only $I(\pi)/I_F = 0.26$. Still, most of the emission is concentrated in the main lobe around $\theta = 0$, with much smaller sidelobes around $\theta = \pm 1.29$ (74°). However, the losses have widened the main lobe to a half angle of $\theta_{1/2} = 1.06$ (61°), an increase of about 15 %. Thus the enhancement of emission in the forward direction is considerably decreased, but the overall emission pattern is nearly unchanged. It should therefore be possible to build a working nano-optical Yagi-Uda antenna from the 100 nm long gold nanorods discussed at the end of section 4.

As losses increase, the emission pattern gradually blurs. Fig. 7 shows the emission pattern for a Yagi-Uda antenna with $\gamma_n = 1$ for all elements. The director detuning is $\delta = 2$ and the array spacings are $x_r = -1.4$ and $x_a = 2$. The enhancement of forward emission has now dropped to $I(0)/I_F = 2.3$ and the suppression of backward emission is only $I(\pi)/I_F = 0.45$. The distinction between the main lobe and the side

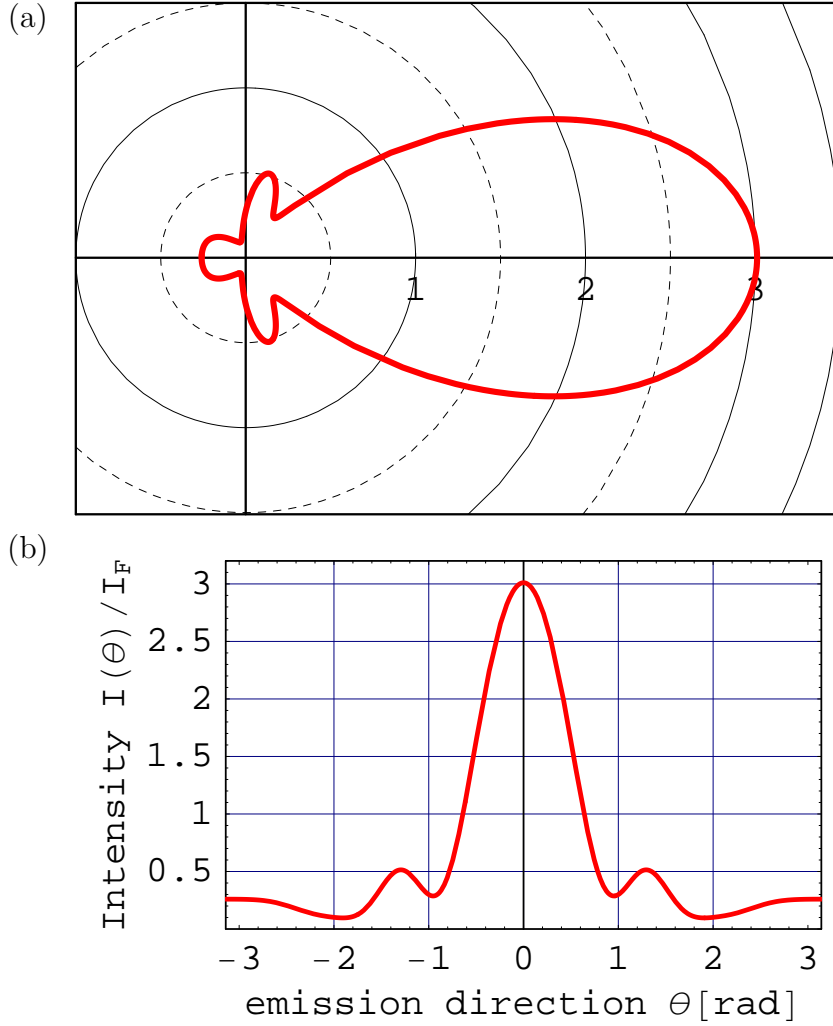


Figure 6. Emission pattern of an antenna with losses equal to $\gamma_n = 0.5$ for each element. (a) shows the polar plot and (b) shows the rectangular plot. The other antenna parameters are $x_r = -1.4$, $x_a = 2$, $\delta = 1.5$.

lobes at $\theta = \pm 1.32$ (76°) begins to wash out and the main lobe has widened to a half angle of $\theta_{1/2} = 1.20$ (69°), an increase of 30 % over the loss free case shown in fig. 3. Interestingly, the emission pattern still has the characteristic features of the Yagi-Uda antenna, despite the rather high emission into side lobes.

8. Conclusions

We have shown that a nano-optical Yagi-Uda antenna can be build from nanoparticles if the absorption losses are sufficiently small compared to the radiation losses. Specifically, a good emission pattern can already be obtained at a loss ratio of $\gamma = 0.5$ (absorption losses equal to half the radiation losses). In general, the loss parameter γ can be reduced by making the nanoparticles larger, so the material properties define a minimal size for

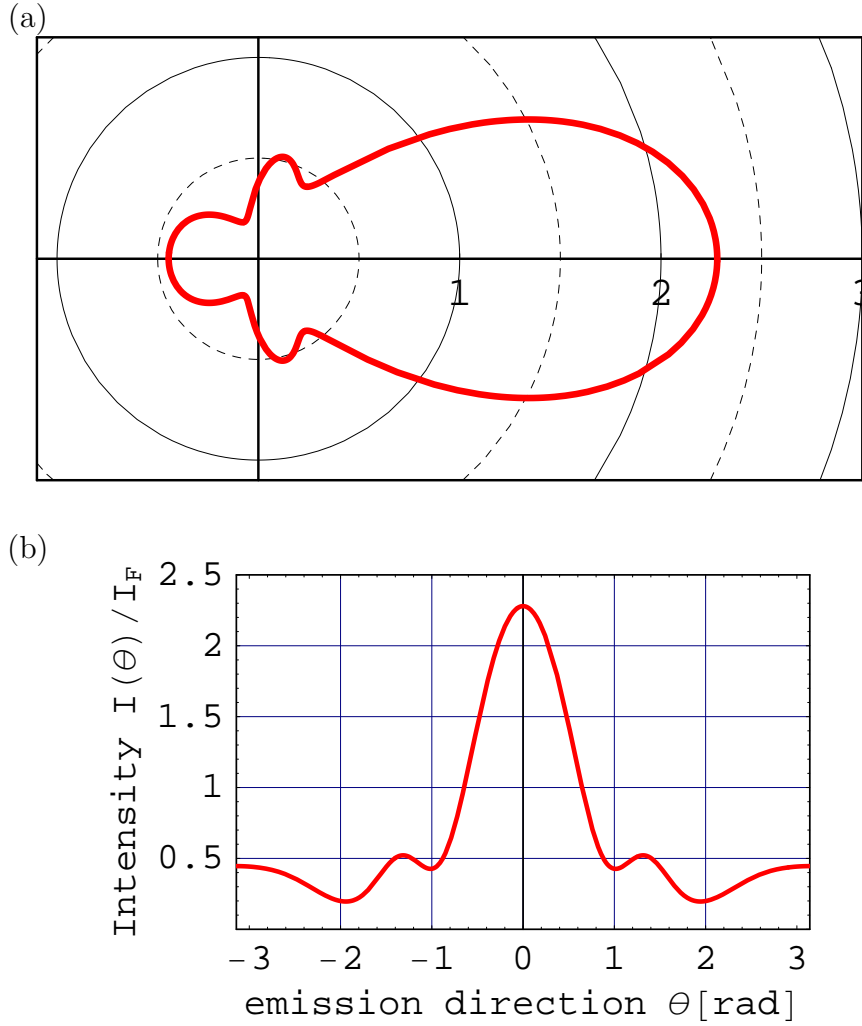


Figure 7. Emission pattern of an antenna with losses equal to $\gamma_n = 1$ for each element. (a) shows the polar plot and (b) shows the rectangular plot. The other antenna parameters are $x_r = -1.4$, $x_a = 2$, $\delta = 2$.

each type of nanoparticle. We have derived the appropriate sizes for gold nanoparticles embedded in a glass matrix, indicating that a loss parameter of $\gamma = 0.5$ can be obtained for elliptical gold nanorods of about 115 nm in length.

It might be worth noting that a somewhat smaller size limit can be obtained for silver nanoparticles. For comparison, the optical response of silver in glass at 705 nm would be described by $\epsilon_r - 1 = 11.2 + i0.14$, corresponding to $\gamma R = 1.12 \times 10^{-3}$, or about one sixth of the losses in a gold particle. However, the general size dependence of losses remains unchanged, so the nanoparticles in an antenna array cannot be made arbitrarily small, regardless of material.

Other design parameters seem to be less critical. In particular, the working principle of the Yagi-Uda antenna is not sensitive to small changes in array spacings and in detuning. We therefore expect nano-optical Yagi-Uda antennas to work even in limits

were the simple dipole approximation used above ceases to apply.

In summary, the absorption losses in nanoparticles need to be taken into account when constructing a nano-optical Yagi-Uda antenna. However, the directionality of light emission from the antenna can be observed even in the presence of non-negligible losses such as the ones expected in gold nanorods. Our results thus indicate that a working nano-optical Yagi-Uda antenna could be realized by an array of 100 nm gold nanorods embedded in a glass substrate.

Acknowledgments

Part of this work has been supported by the Grant-in-Aid program of the Japanese Society for the Promotion of Science and the Furukawa technology foundation.

- [1] Engheta N, Salandrino A, and Alu A 2005 *Phys. Rev. Lett.* **95** 095504
- [2] Maier S A and Atwater H A 2005 *J. Appl. Phys.* **98** 011101
- [3] Gersen H, Garcia-Parajo M F, Novotny L, Veerman J A, Kuipers L and van Hulst N F 2000 *Phys. Rev. Lett.* **00** 5312
- [4] Greffet J J 2005 *Science* **308** 1561
- [5] Schuck P J, Fromm D P, Sundaramurthy A, Kino G S and Moerner W E 2005 *Phys. Rev. Lett.* **94** 017402
- [6] Mühlischlegel P, Eisler H-J, Martin O J F, Hecht B and Pohl D W 2005 *Science* **308** 1607
- [7] Farahani J N, Pohl D W, Eisler H J and Hecht B 2005 *Phys. Rev. Lett.* **95** 017402
- [8] Cubukcu E, Kort E A, Crozier K B and Capasso F 2006 *Appl. Phys. Lett.* **89** 093120
- [9] Kosako T, Yamashita T, Hofmann H F and Kadoya Y 2006 *Extended abstracts of the 67 th autumn meeting of the Japan Society of Applied Physics, August 28th to September 1st 2006, Kusatsu, Japan* p 943
- [10] Li J, Salandrino A and Engheta N 2007 *e-print cond-mat/0703086*
- [11] Johnson P B and Christy R W (1972) *Phys. Rev. B* **6**, 4370
- [12] Sun L, Hao Y, Chien C L and Searson P C 2005 *IBM J. Res. & Dev.* **49**, 79
- [13] Markel V A 1993 *J. Mod. Opt.* **40** 2281
- [14] Zou S and Schatz G C 2006 *Nanotechnology* **17** 2813